A Precursor to the Solvent Radical Cation MCH^+: Pulse Radiolysis of Liquid Methylcyclohexane (MCH) at 143 K

R. E. Bühler*,† and Y. Katsumura‡

Laboratory for Physical Chemistry, Swiss Federal Institute of Technology, ETH-Zürich, Switzerland

Received: June 25, 1997; In Final Form: October 3, 1997[⊗]

It is shown by pulse radiolysis that in N_2O-saturated methylcyclohexane (MCH) the solvent radical cation MCH^+ is formed, but in argon-saturated MCH, the olefinic fragment cation methylcyclohexene$^+$ (MCHexene$^+$) is obtained. From simulations of the geminate ion kinetics with the $t^{-0.6}$ semiempirical rate law, it is concluded that both cations must have a common precursor: some excited state of MCH^+, called M^+*. This precursor either fragments to form MCHexene$^+$ or is quenched, e.g. by N_2O, to form MCH^+, or relaxes in the MCH environment. The corresponding rate constants at 143 K are $k_{frag} = (2.5 \pm 0.5) \times 10^6\ s^{-1}$, $k_2(M^+* + N_2O) = (3.1 \pm 0.5) \times 10^7\ M^{-1}\ s^{-1}$ and $k_0 = (3.2 \pm 1.6) \times 10^5\ s^{-1}$. The mobility of M^+* was assumed to correspond to that of the fast MCH^+, i.e. $D_{M^{+}*} \approx D_{MCH^+} = (1.8 \pm 0.2) \times 10^{-6}\ cm^2\ s^{-1}$. The mobility of the solvated electron, $D_{e^-_{solv}}$, was determined to be $(1.6 \pm 0.2) \times 10^{-6}\ cm^2\ s^{-1}$. From a Lorentzian line shape analysis of the free ion intercept spectra, the individual yields for both systems were derived. The optimal line parameters are the following: for MCH^+ $\lambda_{max} = 570$ nm, hwhm (half-width at half-maximum) = 19000 cm^{-1}; for MCHexene$^+$ $\lambda_{max} = 450$ nm, hwhm = 5500 cm^{-1}; and for e^-_{solv} $\lambda_{max} = 1900$ nm, hwhm = 4500 cm^{-1}. Using the known free ion yield ($G_{fi} = 0.06 \pm 0.015$ (100 eV)$^{-1}$) the absorption coefficients are calculated to be: $\epsilon(MCHexene^+)_{450nm} = 2260 \pm 200\ M^{-1}\ cm^{-1}$, $\epsilon(MCH^+)_{570nm} = 1910 \pm 150\ M^{-1}\ cm^{-1}$, $\epsilon(e^-_{solv})_{700nm} = 1100 \pm 50\ M^{-1}\ cm^{-1}$, and $\epsilon(M^+*)_{600nm} = 700 \pm 50\ M^{-1}\ cm^{-1}$. The error limits given are due to the line shape analysis only. There is an additional systematic effect due to the error-limit for the G_{fi}-value (±25%): all ϵ-values become higher if the G_{fi}-value should be smaller.

Introduction

Recently we have shown by pulse radiolysis that the transient absorption in N_2O-saturated or CO_2-saturated methylcyclohexane (MCH), peaking at about 570 nm, is due to the solvent radical cation MCH^+.[1,2] From simulations using the semiempirical $t^{-0.6}$ rate law for geminate ion recombinations,[1,3] it was concluded that MCH^+ is of very high mobility: about 400 times faster at 133 K than expected from diffusion. At room temperature it is about 11 times faster than diffusion, in very good agreement with the conductivity data from Warman et al.[4] Estimates for the absorption coefficient and the free ion yield at about 143 K were given.

For a long time Trifunac et al. have published arguments that the high mobility should be assigned to a proton transfer mechanism.[5] More recently, a new interpretation has been given.[6a] Their new model with conformational changes (or effects of impurities[6b]) is not needed to explain our results. The present paper now concentrates on the findings that there must be some precursor species to the radical cation MCH^+ clearly seen from deviations from the expected $t^{-0.6}$ linearity at very early times ($t^{-0.6} > 1.5\ \mu s^{-0.6}$, i.e. $t < 500$ ns). Initially these deviations were thought to be due to validity limitations of the semiempirical $t^{-0.6}$ rate law for very early times. However, after having studied a large variety of systems[7] with similar deviations from linearity, a chemical reason was found for the deviations in all cases. More recently, theoretical support was given by Barczak and Hummel[8] in favor of a wider validity of the $t^{-0.6}$ rate law. Further agruments for the existence of a precursor species to the radical cation stems from experiments with neat MCH (actually argon-saturated MCH) in which the olefinic cation of methylcyclohexene (MCHexene$^+$) was found to replace the high mobility radical cation MCH^+.

The aim of the present paper is to give proof for the existence of a precursor species to the radical cation MCH^+. This precursor either relaxes (or is quenched) to MCH^+ or fragments to form the olefinic cation. Pulse radiolysis experiments with N_2O-saturated and argon-saturated MCH at 143 K (−130 °C) allowed us to characterize this precursor and to determine the quenching rate and fragmentation rate. It is proposed that this precursor must correspond to some excited state of the radical cation MCH^+, which we call M^+*.

Experimental Section

Pulse Radiolysis. The technique of pulse radiolysis with a Febetron 705 accelerator (Physics International) for 30 ns pulses of 2 MeV electrons has been used as reported.[9,10] All experiments were performed at 143 K (−130 °C) in the liquid state (due to the MCH melting point of 146.5 K it is a supercooled liquid state). The stainless steel cell had an optical path length of 2 cm. A typical dose was between 50 and 150 Gy. Dosimetry was done by calorimetry. The data treatment, kinetic analysis, and data simulation were performed on a PDP 11/73 computer. In the $t^{-0.6}$ linearity tests, as shown, e.g. in Figure 1, there are usually three different experimental curves from a single photomultiplier. They cover three different,

† Mailing address: Physical Chemistry, ETH Zürich, Mühlebachstr. 96, 8008 Zürich, Switzerland.

‡ Permanent address: Nuclear Engineering Research Laboratory, Faculty of Engineering, University of Tokyo, Bunkyo-ku, Tokyo, Japan.

⊗ Abstract published in *Advance ACS Abstracts,* December 1, 1997.

S1089-5639(97)02065-3 CCC: $15.00 © 1998 American Chemical Society
Published on Web 01/01/1998

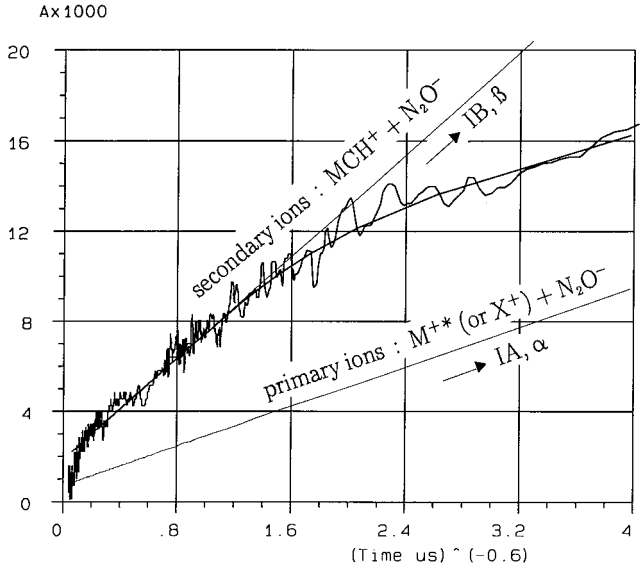

Figure 1. $t^{-0.6}$ plot of the rate curve at 550 nm for N_2O-saturated MCH at 143 K (−130 °C). A = absorbance at 100 Gy. Parameters of the primary ions are $\alpha = 3.05\ \mu s^{0.6}$, intercept IA = 0.72×10^{-3}; of the secondary ions[1] $\beta = 3.05\ \mu s^{0.6}$, intercept IB = 1.85×10^{-3}; and the first-order rate constant $k_1 = 6.1 \times 10^6\ s^{-1}$.

partially overlapping time ranges and are from two different transient digitizers: Tektronix 7912AD or 2440 and Datalab DL912.

Cell Window Signal. Although the quartz windows of the cell were of highest purity (Suprasil), the production of color centers in the quartz windows introduce additional small absorptions, particularily at low temperatures. The correction is important for the rate curve analysis. It affects seriously the intercepts from the $t^{-0.6}$ linearity and therefore the free ion spectra. For all temperatures and wavelengths used in the experiments, the cell signal (quartz defects) was determined as described in the previous paper.[1]

Shock Wave Disturbances. The origin of shockwaves in pulse radiolysis cells and the methods to minimize the effect have previously been discussed in detail.[1,9] The amount of disturbance on the transient absorption signal is dependent on the optical characteristics of the solution. As the patterns are correlated with the speed of sound, the shock signals can be identified at earlier times, but get smeared out later on. In Figure 1 typical weak shock signals may be seen at $t^{-0.6} \approx 0.4$ and 0.6 $\mu s^{-0.6}$ (for a clearer example with stronger effects, see Figure 5 in ref 1).

Chemicals. Methylcyclohexane (Fluka purum, >98 % GC) was passed through a column of aluminum oxide, dried over molecular sieve A4, and then fractionated through a Fischer "Spaltrohrkolonne" with about 30 theoretical plates. N_2O (99 %) and argon (99.996 %) were from PanGas Luzern.

Simulation of Geminate Ion Kinetics

As in the previous paper[1] the geminate ion kinetics is simulated by the $t^{-0.6}$ rate law by van den Ende et al.[3] It describes the probability of survival of the geminately recombining ions relative to the free ion yield:

$$\frac{G(t)}{G_{fi}} = 1 + \underbrace{0.6\left[\frac{r_c^2}{D}\right]^{0.6}}_{\alpha} t^{-0.6} = \frac{\text{absorbance}(t)}{\text{absorbance}(\infty)} = \frac{A(t)}{IA} \quad (1)$$

The absorption may have contributions from both types of ions (sum of both absorption coefficients). Any plot of the absorbance $A(t)$ against $t^{-0.6}$ should be linear. Its intercept IA for $t = \infty$ corresponds to the absorbance of the free ion yield. The slope divided by the intercept IA is called α. From this value, with the known Onsager radius r_c, an experimental diffusion constant can be derived: $D_{exp} = D^+ + D^-$. Theoretical support for the $t^{-0.6}$ rate law was recently given by Barczak and Hummel.[8]

If geminate ions undergo reactions, there are two limiting rate laws: At very early times, the geminate recombination is between the primary ions only

$$\frac{A_{prim}(t)}{IA} = 1 + \alpha t^{-0.6} \quad \text{with} \quad \alpha = 0.6\left[\frac{r_c^2}{D_{prim}}\right]^{0.6} \quad \text{and} \quad IA = A_{prim}(\infty) \quad (2)$$

At very late times the geminate recombination is between the secondary ions only

$$\frac{A_{sec}(t)}{IB} = 1 + \beta t^{-0.6} \quad \text{with} \quad \beta = 0.6\left[\frac{r_c^2}{D_{sec}}\right]^{0.6} \quad \text{and} \quad IB = A_{sec}(\infty) \quad (3)$$

The changeover from the primary to the secondary pair of geminate ions is due to a first-order reaction (e.g. fragmentation) or to a pseudo-first-order scavenging process. The *primary ion kinetics* with k_1 as a first-order or pseudo-first-order rate constant is therefore given by

$$\frac{A_{prim}(t)}{IA} = [1 + \alpha t^{-0.6}]e^{-k_1 t} \quad (4)$$

The *secondary geminate ion kinetics* is approximated by

$$\frac{A_{sec}(t)}{IB} = [1 + \beta t^{-0.6}][1 - e^{-k_1 t}] \quad (5)$$

The sum of the primary and secondary ion absorbances then simulates the experimental time profile

$$A(t) = A_{prim}(t) + A_{sec}(t) \quad (6)$$

A discussion of the accuracy and the characteristics of the $t^{-0.6}$ kinetic plots was given in the previous paper.[1] The $t^{-0.6}$ linearity simulates the geminate ion kinetics only. The free ion recombination therefore shows up as a deviation from linearity at late times. In this paper this is about $t^{-0.6} < 0.2\ \mu s^{-0.6}$ or $t >$ ca. 15 μs (143 K).

The parameter fitting for geminate ion kinetics with an overlying ionic reaction should again follow the sequence as illustrated in our earlier paper:[1] (A) The secondary ion kinetics (β-value and intercept IB) is determined directly from the linearity at late times. (B) The deviation from that linearity toward earlier times is primarily dependent on k_1. (C) The very early part then is defined by the primary ion kinetics (α-value and intercept IA). If α is known from other experiments, then the fitting determines IA, or vice versa. If both parameters are not known, the parameter determination is difficult.

The accuracy of the α- or β-values and of the derived diffusion constants D_{exp} from the kinetic analysis with the $t^{-0.6}$

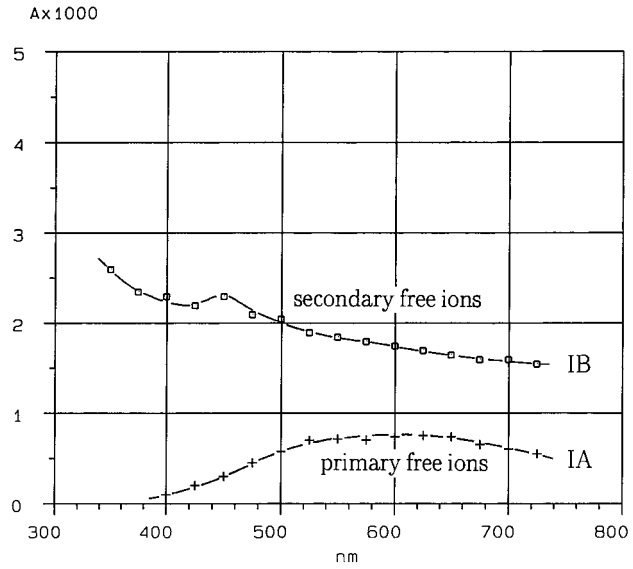

Figure 2. Free ion intercept spectra for N_2O-saturated MCH at 143 K (−130 °C). A = absorbance at 100 Gy. IA for the primary pairs of ions (M^{+}* (or X^{+}) + N_2O^{-}) and IB for the secondary pair of ions (MCH^{+} + N_2O^{-}).

rate law is critically dependent on the error limits of the rather small intercepts. This is due to the very small free ion yield for nonpolar solvents at low temperatures.[1] In this paper α- or β-values are averaged over the relevant wavelength range, typically 400 nm < λ < 750 nm. The intercept spectra then are derived with the mean values of α or β.

Results

N_2O-Saturated MCH. In the previous paper[1] this system was investigated for $t > 0.5\ \mu s$ ($t^{-0.6} < 1.5\ \mu s^{-0.6}$). The kinetic plot against $t^{-0.6}$ was linear for $0.2 < t^{-0.6} < 1.2\ \mu s^{-0.6}$ with $\beta = 3.05\ \mu s^{0.6}$, revealing a high-mobility cation MCH^{+} with $D_{MCH^{+}}$ (143 K) = (1.8 ± 0.2) × 10^{-6} $cm^2\ s^{-1}$. The corresponding free ion intercept spectrum IB is included again in Figure 2. In the previous paper[1] β and IB were called α and IA as MCH^{+} and N_2O^{-} were treated as the primary pair of geminate ions. In this paper they represent the secondary pair of ions. As shown in Figure 1 there is a build up for the MCH^{+} absorption for $t^{-0.6} > 1.5\ \mu s^{-0.6}$, a deviation from the $t^{-0.6}$ linearity toward smaller absorption for larger $t^{-0.6}$ values, i.e. at earlier times.

Such deviations originally were thought as being due to the limited validity of the semiempirical $t^{-0.6}$ kinetic rate law. However today, after having studied dozens of systems[7] with nearly thousands of rate curves, we are convinced that in our low-temperature studies the $t^{-0.6}$ rate law holds up to at least $t^{-0.6} \approx 4\ \mu s^{-0.6}$. This corresponds to our technical time resolution of ca. 100 ns. The buildup in Figure 1 therefore must be real. In other words, the solvent radical cation MCH^{+} is not a direct product from the irradiation pulse. There must be a positively charged precursor X^{+} and the corresponding reaction mechanism follows Scheme 1.

β and IB were determined in the previous paper.[1] From the point of deviation from linearity (from $t^{-0.6} \approx 1.2\ \mu s^{-0.6}$) toward earlier times (larger $t^{-0.6}$-values) the rate constant k_1 is derived. From the amount of deviation (for $t^{-0.6} > 2.5\ \mu s^{-0.6}$) the parameters α and IA may be determined. They are, however, coupled. Unless one of the two parameters is accessible by other ways, there is little hope to resolve the individual parameters α and IA.

SCHEME 1

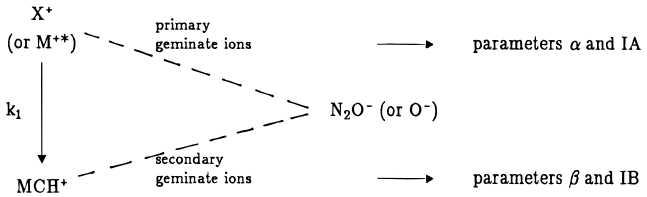

It might be expected that the precursor of a high-mobility radical cation MCH^{+} is also of a similar high mobility. We checked mobilities for X^{+} from 10 times faster to 10 times slower than $D_{MCH^{+}}$, without finding an obvious criteria, except that for larger α the intercept spectrum IA becomes smaller with the same band shape. It was therefore assumed that the precursor X^{+} has the same high mobility as MCH^{+}:

$$D_{X^{+}} \approx D_{MCH^{+}} = 1.8 \times 10^{-0.6}\ cm^2\ s^{-1}$$

This assumption has no influence on the rate constant k_1. α becomes identical to $\beta = 3.05\ \mu s^{0.6}$ and the corresponding IA revealed the free ion spectrum of the primary pair of geminate ions. As the anion N_2O^{-} (or O^{-}) does not absorb in the visible λ-range, the IA-spectrum, shown in Figure 2, represents the spectrum of the precursor X^{+} alone.

Since X^{+} is precursor to the solvent radical cation, it is difficult to propose anything else than X^{+} to be some excited state of MCH^{+}. To indicate this likely interpretation, X^{+} is now called M^{+}*.

The rate of relaxation from M^{+}* to MCH^{+} is derived from 450 nm < λ < 750 nm to be

$$k_1 = (6.1 \pm 0.3) \times 10^{6}\ s^{-1}$$

For $\lambda \leq 450$ nm, k_1 appears to drop by 15−25% (at 375 nm), probably due to overlapping UV-absorptions. The secondary spectrum IB (Figure 2) is due to the radical cation MCH^{+} with some contribution from the olefinic fragment cation: methylcyclohexene^{+} as discussed in the previous paper.[1] As there is no contribution of the MCHexene^{+} (450 nm band) in the precursor spectrum (IA), M^{+}* must also be precursor to MCHexene^{+}.

Argon-Saturated MCH. Generally the intercepts from $t^{-0.6}$-plots, corresponding to the free ion yield ($G_{fi} = 0.06 \pm 0.015$ $(100\ eV)^{-1}$) are extremely small and often not of the accuracy needed to derive good α- and β-values (see N_2O-saturated MCH). The only way to increase the intercepts is to choose ions of larger absorption coefficients. With this idea in mind, experiments with neat MCH (actually argon-saturated MCH) were studied. The negative charge then appears as a solvated electron with a strong absorption toward the near-infrared. The experimental result (Figure 3), however, showed that the MCH^{+}-absorption was mostly replaced by a strong 450 nm band. At very early times (e.g. at 0.15 μs) there are two absorption bands in addition to the absorption of the solvated electron: a 450 nm band, corresponding to the band of the olefinic cation (MCHexene^{+}), as in the N_2O-saturated solution, and a weaker band at ca. 550 nm. The latter disappears rather rapidly, whereas the 450 nm species initially decays much slower until all 550 nm absorption has disappeared. At late times ($t \geq 1.5\ \mu s$) the 450 nm band and the spectrum of e^{-}_{solv} disappear in parallel, as found from the linear slow part of the $t^{-0.6}$-plots in Figure 4. The detailed analysis of the rate curves by the $t^{-0.6}$ rate law reveals, in first approximation, the mechanism of Scheme 2.

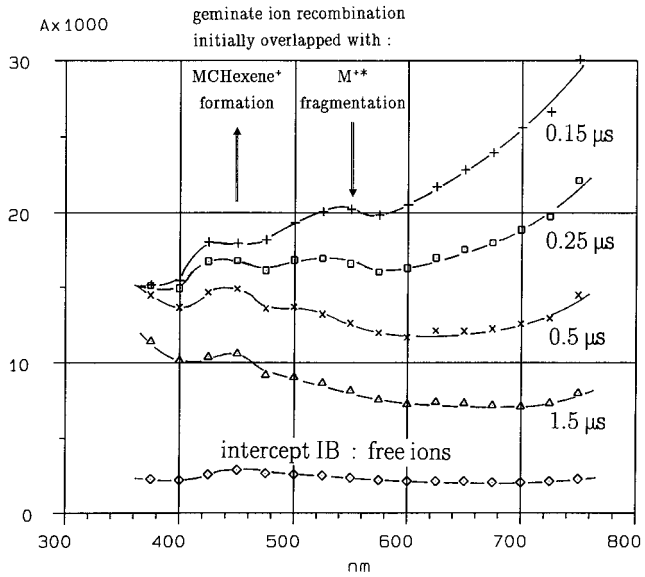

Figure 3. Early transient spectra in argon-saturated MCH at 143 K (−130 °C) and the secondary free ion intercept spectrum IB for comparison. A = absorbance at 100 Gy.

The typical rate curve simulations are shown in Figure 4. They are representative for the complete λ-range from 375 to 750 nm. For λ < 650 nm the deviation at early times from the late $t^{-0.6}$ linearity is toward smaller absorbances, whereas for λ > 650 nm it is toward higher absorbances. The slow linear part ($t^{-0.6} \leq 1.0\ \mu s^{-0.6}$) yields $\beta = 3.2 \pm 0.2\ \mu s^{0.6}$ (averaged over all λ) with $D_\beta = (1.6 \pm 0.2) \times 10^{-6}$ cm^2 s^{-1} and the corresponding intercept spectrum IB(λ) as seen in Figure 5. D_β reveals that the mobility of the secondary geminate ions (450 nm species + e^-_{solv}) is slower than the radical cation MCH^+, although the solvated electron is of high mobility. This indicates that the 450 nm band must be due to a slow cation recombining with the fast e^-_{solv}. The diffusion constant $D_\beta = 1.6 \times 10^{-6}$ cm^2 s^{-1} derived from $\beta = 3.2\ \mu s^{0.6}$ is therefore reflecting the mobility of the solvated electron, and the 450 nm is due to the olefinic fragment cation from MCH^+:[11] the methylcyclohexene$^+$. It must move by diffusion, and the high D_β-value must correspond exclusively to the mobility of the solvated electron:

$$D_{e^-_{solv}}(143\ \text{K}) = (1.6 \pm 0.2) \times 10^{-6}\ \text{cm}^2\ \text{s}^{-1}$$

With this value and the assumed diffusion constant of the precursor M^{+}*, it is possible to derive an α-value for the primary pair of geminate ions:

$$\text{with} \qquad D_\alpha = D_{e^-_{solv}} + D_{M^{+*}} = (3.4 \pm 0.6) \times 10^{-6}\ \text{cm}^2\ \text{s}^{-1}$$

$$\text{follows} \qquad \alpha = 2.1 \pm 0.2\ \mu s^{0.6}$$

With this result the simulation of the early part of the $t^{-0.6}$ plot from 375 nm < λ < 750 nm yields a fragmentation rate constant of

$$k_1 = (3.2 \pm 0.2) \times 10^6\ \text{s}^{-1}$$

and the free ion intercept spectrum IA(λ), as shown in Figure 5.

If the assumed value $D_{M^{+*}}$ should be smaller, α becomes larger and correspondingly IA(λ) becomes smaller (same effect as in the N_2O-saturated system). It has no effect on the fragmentation rate constant k_1.

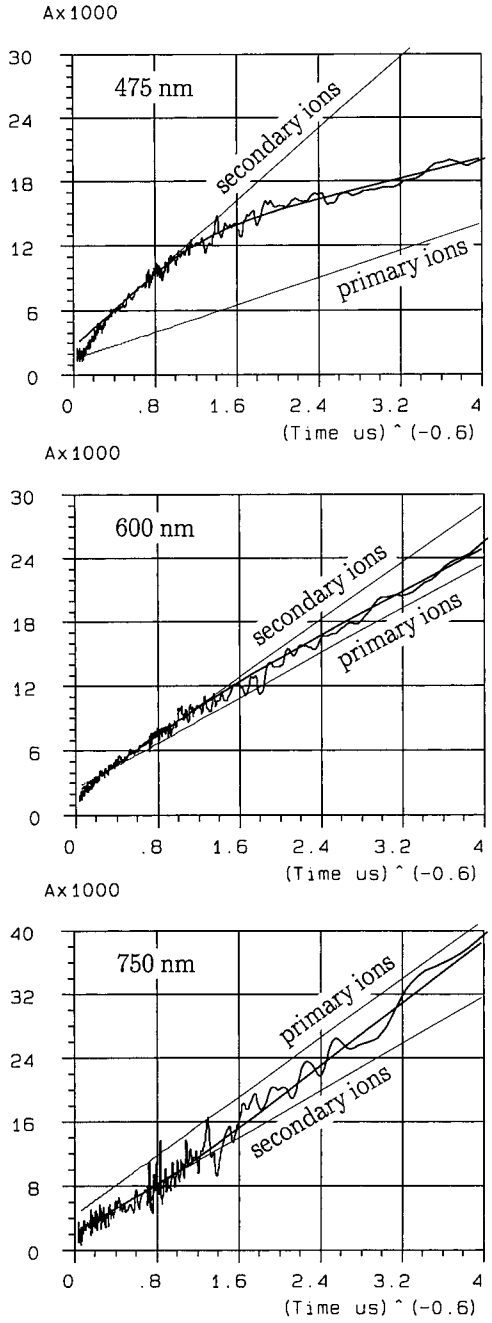

Figure 4. $t^{-0.6}$ plot of the rate curves at 475, 600, and 750 nm for argon-saturated MCH at 143 K (−130 °C). A = absorbance at 100 Gy. Parameters are $\alpha = 2.1\ \mu s^{0.6}$ for the primary pair of ions and $\beta = 3.2\ \mu s^{0.6}$ for the secondary pair of ions. For the intercepts IA and IB, see Figure 5. The rate constant is $k_1 = 3.2 \times 10^6$ s^{-1}.

SCHEME 2

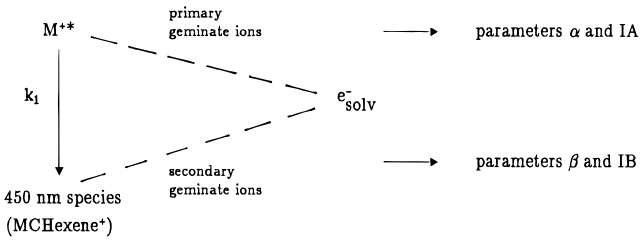

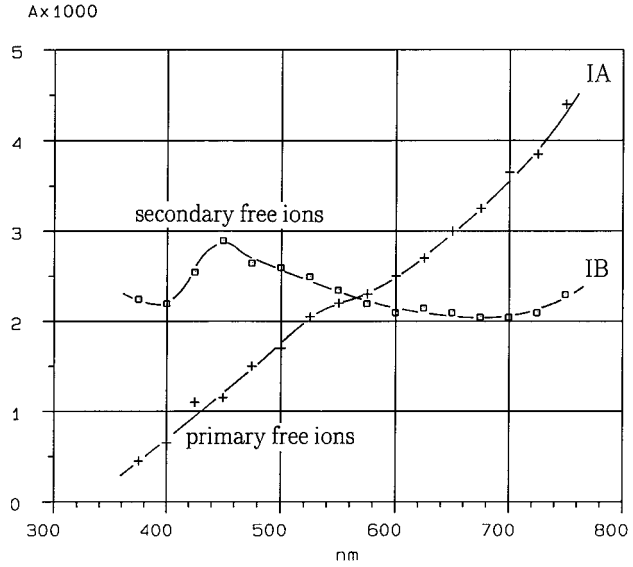

Figure 5. Free ion intercept spectra for argon-saturated MCH at 143 K (−130 °C). A = absorbance at 100 Gy. IA for the primary pair of ions (M^{+}* (or X^{+}) + e^{-}_{solv}) and IB for the secondary pair of ions (MCHexene^{+} + e^{-}_{solv}).

SCHEME 3

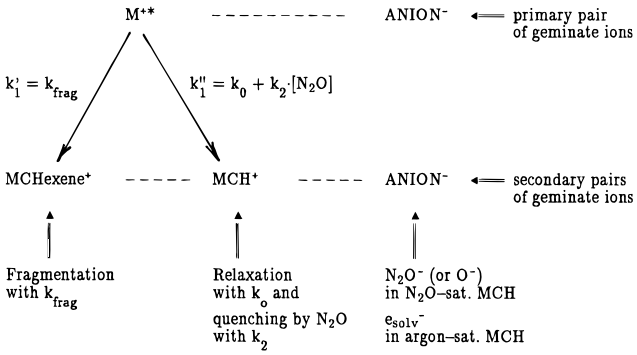

Discussion

The Complete Reaction Model. Whether MCH is saturated with N_2O or with argon, the first-order reaction observed is due to two competing channels leading from the precursor M^{+}* either to the relaxed solvent radical cation MCH^{+} or to the fragment cation MCHexene^{+}. The electron scavenger N_2O obviously simultaneously acts as a quencher for the precursor species: Scheme 3.

As seen in Figure 2 for the N_2O-saturated system, there is some contribution to the spectrum from MCHexene^{+} (additional to MCH^{+}). In the argon-saturated system, the MCHexene^{+} absorption is dominant (together with the e^{-}_{solv}-absorption) (Figure 5); however, it is difficult to detect a contribution from MCH^{+} (relaxation channel). As the secondary geminate ions are made up of two pairs (MCHexene^{+}/anion^{-} and MCH^{+}/anion^{-}) with different diffusion constants D_β, the β-values are expected to be λ-dependent, somewhat weighed by the absorption coefficients. In both systems no such λ-dependence could be detected. It appears to be small, as one reaction channel is always dominant. The effect therefore must be hidden within the experimental error limits.

Lorentzian Line Shape Analysis. For a discussion of the relative contributions of the two channels, a line shape analysis was introduced. As the intercept spectra from the $t^{-0.6}$ linearities correspond to the free ion yield (G_{fi} = 0.06 ± 0.015 (100 eV)$^{-1}$)[1] there is a quantitative base for this discussion.

TABLE 1: Parameters Used for the Lorentzian Line Shape Analysis

species	λ_{max} (nm)	hwhm (cm^{-1})	hwhm (nm) UV-side	absorbance × 1000 at λ_{max} and for 100 Gy: N_2O-sat. MCH	absorbance × 1000 at λ_{max} and for 100 Gy: argon-sat. MCH
MCH^{+} [1]	570	19000	300	1.3 ± 0.1	0.2 ± 0.1
MCHexene^{+} [11]	450	5500	90	0.90 ± 0.05	2.2 ± 0.1
e^{-}_{solv} [13,14]	1900	4500	870		8.7 ± 0.4
	700[a]				1.2 ± 0.1
M^{+}* [b]	600	5300	145	0.75 ± 0.05	1.65 ± 0.10

[a] Reference wavelength for ϵ-calculation (not λ_{max}). [b] Derived from the intercept spectra of the primary geminate ions (see text).

All line shapes were taken as Lorentzian (in analogy to collisional broadening in high-density systems.[12] The λ_{max} were taken from experiments: 570 nm for MCH^{+},[1] particularly supported by the early transient spectra, as seen in Figure 2a of ref 1; 450 nm for MCHexene^{+} in analogy to cyclohexene^{+} as measured in a MCH-solution of cyclohexene (and N_2O) at 143 K;[11] and 1900 nm for the solvated electron as measured at 163 K by Baxendale et al.[13] The half-widths at half-maximum (hwhm, on UV-side given in nm) were allowed to vary within experimentally allowed limits: from 220 nm to 300 nm for MCH^{+}, from 70 to 90 nm for MCHexene^{+}, and from 800 to 900 nm for e^{-}_{solv}. The actual simulation for e^{-}_{solv} was fitted to the experimental spectrum found in an MCH-solution of TEA (triethylamine) at 143 K[14] in the range 450 nm < λ < 650 nm. The simulation then allowed the extrapolation down to 350 nm and up to 750 nm. The final best simulation is based on the parameters as given in Table 1.

The result of the line shape analysis for the free ion spectra of the secondary geminate ions (intercepts IB) are shown in Figure 6 for the MCH−N_2O-system and in Figure 7 for the MCH−argon-system. In both cases part a gives the individual contributions of MCH^{+}, MCHexene^{+}, and e^{-}_{solv}, whereas part b shows the accuracy test of the simulation. In both systems there is a rather good fit, except for some small unidentified UV-band for λ < 450 nm (Figure 6b) or λ < 400 nm (Figure 7b). The absorbance maxima needed for the line shape analysis are given in Table 1.

Figure 8 displays the results for the free ion spectra of the primary geminate ions (intercepts IA) in N_2O- as well as argon-saturated MCH. For the N_2O-saturated system the intercept spectrum IA directly reveals the spectrum of M^{+}*. This absorption band can be simulated with a Lorentzian line with λ_{max} = 600 nm and hwhm = 5300 cm^{-1} (145 nm on UV-side) (see Table 1). For the argon-saturated system, the intercept spectrum IA (Figure 5) corresponds to the sum of M^{+}* and $e^{-}_{solv.}$ Assuming that the e^{-}_{solv}-spectrum at very early times (needed for IA) is identical to the late spectrum of e^{-}_{solv} (from IB, see Figure 7a), the spectrum of M^{+}* may again be derived (Figure 8). For $\lambda \leq$ 600 nm the line shape is identical to the directly determined M^{+}*-spectrum, however with about twice the absorbance. For λ > 600 nm the deviation indicates that the solvated electron contribution might not be fully compensated. The difference between the two M^{+}*-spectra is actually very comparable again to the e^{-}_{solv}-spectrum. All this indicates that the early and late e^{-}_{solv}-spectrum might differ. It is blieved that the directly determined M^{+}*-spectrum (N_2O-saturated system, curve "a" in Figure 8) is the reliable one.

Competition Yields. If argon is replaced by N_2O in an MCH solution, the yield of MCH^{+} increases and that of MCHexene^{+} reduces by the same amount. From the absorbance changes

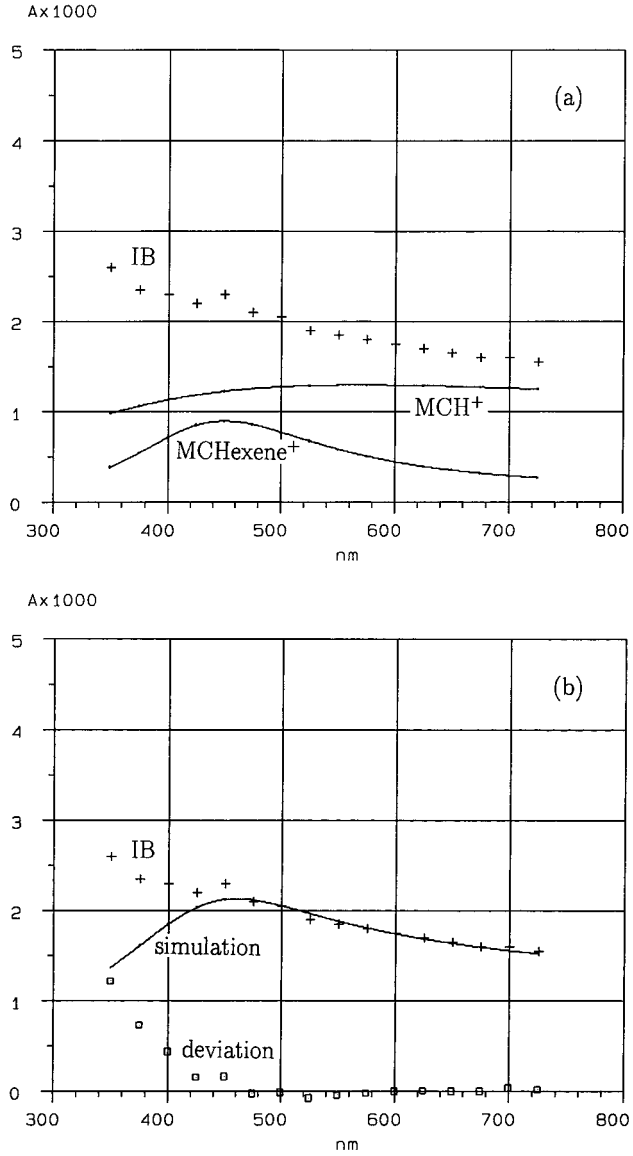

Figure 6. Line shape analysis for the free ion intercept IB (+) in N_2O-saturated MCH, (a) with Lorentzian lines for MCH^+ and $MCHexene^+$ (for parameters, see Table 1), (b) the accuracy test: comparing the sum of the individual Lorentzian lines (—) with IB (+) and showing the deviation (□), with some unidentified UV-band.

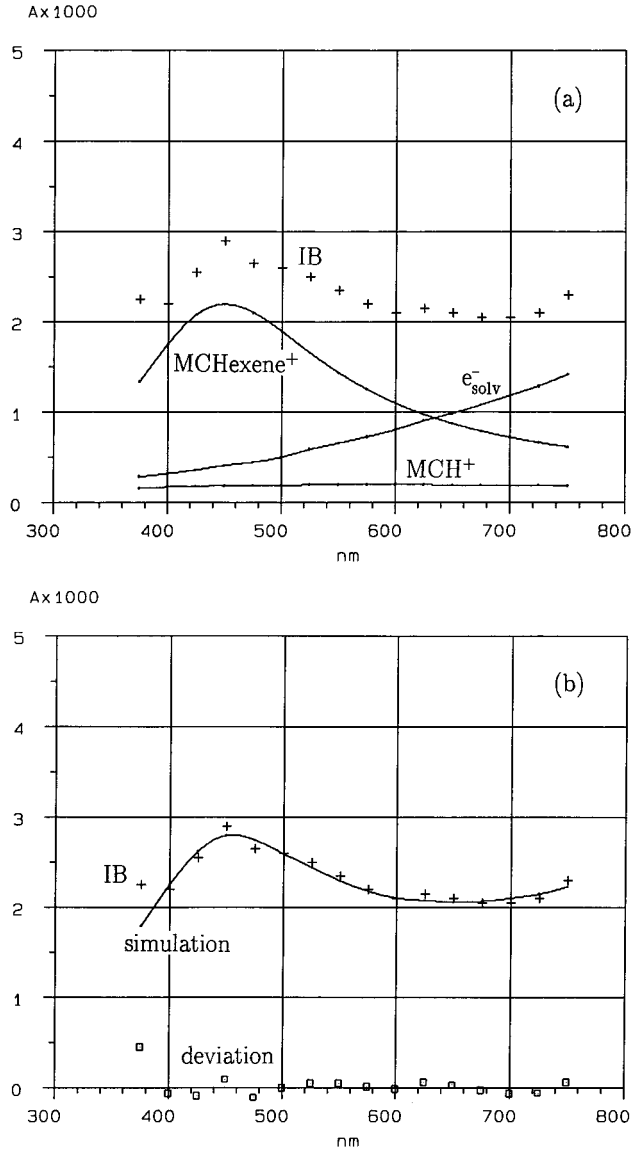

Figure 7. Line shape analysis for the free ion intercept IB (+) in argon-saturated MCH, (a) with the Lorentzian lines for $MCHexene^+$, MCH^+, and e^-_{solv} (for parameters, see Table 1), and (b) the accuracy test: comparing the sum of the individual Lorentzian lines (—) with IB (+) and showing the deviation (□).

given in Table 1, the ratio of the absorption coefficients of the two band maxima are derived to be $\epsilon(MCHexene^+,450\ nm)/\epsilon(MCH^+,570\ nm) = 1.18 \pm 0.04$. With this ratio and the absorbance yields in Table 1 the product yields from the competing channels (Scheme 3) are calculated for the two systems (Table 2).

Rate Data. With the yield data in Table 2 and the experimental first-order rate constants for the two systems, the individual rate constants in Scheme 3 may be derived. For the argon-saturated system, the experimental $k_1 = k_0 + k_{frag} = (3.2 \pm 0.2) \pm 10^6\ s^{-1}$. k_0 corresponds to 10 ± 5 %; therefore

$$k_0 = (3.2 \pm 1.6) \times 10^5\ s^{-1}$$

and

$$k_{frag} = (2.9 \pm 0.3) \times 10^6\ s^{-1}$$

For the N_2O-saturated system, the experimental $k_1 = k_0 + k_2[N_2O] + k_{frag} = (6.1 \pm 0.3) \times 10^6\ s^{-1}$. $k_1 - k_0$ then has to be split following the percent yield in Table 2 to give

$$k_{frag} = (2.14 \pm 0.35) \times 10^6\ s^{-1}$$

and

$$k_2[N_2O] = (3.65 \pm 0.47) \times 10^6\ s^{-1}$$

With $[N_2O] = 0.118$ M (the system is saturated at room temperature),

$$k_2 = (3.1 \pm 0.5) \times 10^7\ M^{-1}\ s^{-1}$$

From the two results for k_{frag} the following average value is derived:

$$\overline{k_{frag}} = (2.5 \pm 0.5) \times 10^6\ s^{-1}$$

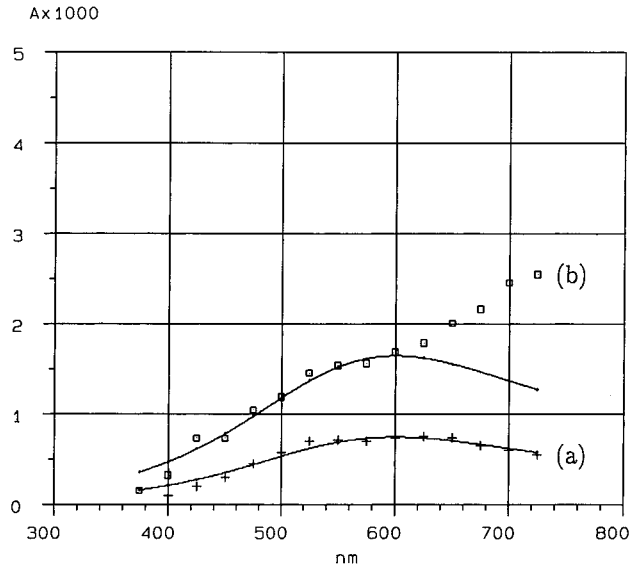

Figure 8. The primary free ion intercept spectra (a) for the N_2O-saturated MCH (+ for IA) and (b) for the argon-saturated MCH corrected for the e^-_{solv} contribution, taken from Figure 7a (□ for IA − $A(e^-_{solv})$). Both results should correspond to the precursor spectrum of M^{+}*. They are both fitted to the same Lorentzian line, however, with different amplitude (parameters in Table 1). Curve a is expected to be the correct spectrum (see text).

Absorption Coefficients. As the intercept spectra correspond to the free ion yield, $G_{fi} = 0.06 \pm 0.015$ (100 ev)$^{-1}$, the absorbance data in Table 1 allow the derivation of absorption coefficients. If one disregards the error limit of G_{fi} the following values result:

$$\epsilon(\text{MCHexene}^+)_{450\text{nm}} = 2260 \pm 200\ \text{M}^{-1}\ \text{cm}^{-1}$$

$$\epsilon(\text{MCH}^+)_{570\text{nm}} = 1910 \pm 150\ \text{M}^{-1}\ \text{cm}^{-1}$$

$$\epsilon(e^-_{solv})_{700\text{nm}} = 1100 \pm 50\ \text{M}^{-1}\ \text{cm}^{-1}$$

From the primary ion intercept IA (Figure 8a) the absorption coefficient of M^{+}* is also available:

$$\epsilon(M^{+}*)_{600\text{nm}} = 700 \pm 50\ \text{M}^{-1}\ \text{cm}^{-1}$$

TABLE 2: Product Yields, Defining the Competition Ratios in Scheme 3

product	channel	N_2O-sat. MCH (%)	argon-sat. MCH
$MCHexene^+$	fragmentation	36.9 ± 3.1	90 ± 5
MCH^+	relaxation	63.1 ± 3.1	10 ± 5[a]

[a] As MCH^+ has a very broad band, curve fitting is rather unspecific.

The error limits given are due to the line shape analysis only. There is an additional systematic effect due to the error limit of the G_{fi}-value (±25 %). A lower G_{fi}-value results in higher ϵ-values throughout (they are inverse proportional to G_{fi}).

Acknowledgment. Support by the Swiss National Science Foundation and by the Research Funds of the ETH is gratefully acknowledged.

References and Notes

(1) Katsumura, Y.; Azuma, T.; Quadir, M. A.; Domazou, A. S., Bühler, R. E., *J. Phys. Chem.* **1995**, *99*, 12821.

(2) Bühler, R. E. *Can. J. Phys.* **1990**, *68*, 918.

(3) van den Ende, C. A. M.; Warman, J. M.; Hummel, A.; *Radiat. Phys. Chem.* **1984**, *23*, 55.

(4) Warman, J. M. In *The Study of Fast Processes and Transient Species by Electron Pulse Radiolysis*; Baxendale, J. H., Busi, F., Eds.; NATO Advanced Study Institute, Reidel Publ. Co.: Dordrecht, NL, 1982; p 433 ff.

(5) As a selection: Trifunac, A. D.; Sauer, M. C.; Jonah, C. D. *Chem. Phys. Lett.* **1985**, *113*, 316. Werst, D. W.; Trifunac, A. D. *J. Phys. Chem.* **1988**, *92*, 1093. Werst, D. W.; Bakker, M. G.; Trifunac, A. D. *J. Am. Chem. Soc.* **1990**, *112*, 40. Sauer, M. C.; Werst, D. W.; Jonah, C. D.; Trifunac, A. D. *Radiat. Phys. Chem.* **1991**, *37*, 461.

(6) (a) Sauer, M. C.; Shkrob, I. A.; Yan, J.; Schmidt, K.; Trifunac, A. D. *J. Phys. chem.* **1996**, *100*, 11325. (b) Shkrob, I. A.; Sauer, M. C.; Schmidt, K. H.; Liu, A. D.; Yan, J.; Trifunac, A. D. *J. Phys. Chem. A* **1997**, *101*, 2120 and references therein.

(7) Bühler, R. E.; et al. Manuscript in preparation.

(8) Bartczak, W. M.; Hummel, A. *Radiat. Phys. Chem.* **1994**, *44*, 335.

(9) Hurni, B.; Brühlmann, U.; Bühler, R. E. *Radiat. Phys. Chem.* **1975**, *7*, 499.

(10) Gebicki, J. L.; Domazou, A. S.; Cirelli, G.; Bühler, R. E. *J. Phys. Chem.* **1994**, *98*, 9570.

(11) Gebicki, J. L.; Bühler, R. E. Unpublished results, 1989.

(12) See, for example: Baranger, M. In *Atomic and Molecular Processes*; Bates, D. R., Ed.; Academic Press: New York, 1962; p 493 ff.

(13) Busi, F. In *The* Study *of Fast Processes and Transient Species by Electron Pulse Radiolysis*; Baxendale, J. H., Busi, F., Eds. NATO Advanced Study Institute, Reidel Publ. Co.: Dordrecht NL, 1982; p 422.

(14) Katsumura, Y.; Bühler, R. E. Unpublished results, 1984.